EMC3-Eirene simulations of the spatial dependence of the tungsten divertor retention in ASDEX Upgrade

T.Lunt[1], Y.Feng[2], K.Krieger[1], R.Neu[1], H.W.Müller[1], E.Wolfrum[1], M.Willensdorfer[3], M.Wischmeier[1] and the ASDEX Upgrade team[1]

E-mail: tilmann.lunt@ipp.mpg.de
[1]Max-Planck-Institut für Plasmaphysik, EURATOM Association, Boltzmannstr. 2, 85748 Garching, Germany
[2]Max-Planck-Institut für Plasmaphysik, EURATOM Association, Wendelsteinst. 1, 17491 Greifswald, Germany
[3]Institut für Angewandte Physik, Technische Universität Wien, Association EURATOM-ÖAW, 1040 Vienna, Austria

Abstract. The Edge Monte Carlo 3D (EMC3) - Eirene code package is applied to simulate the deuterium plasma and neutral particle as well as the tungsten impurity transport in ASDEX Upgrade. Good agreement is found for the deuterium bulk plasma for an L-mode discharge both in the upstream and downstream profiles. The tungsten concentration in the core is computed for a point source placed at different positions around the outer strike point. Comparing the mean impurity residence time for divertor and main chamber sources yields the divertor retention factor R, which shows a very strong dependence on the location of the source relative to the strike point and also on the discharge parameters. While the tungsten transport is strongly suppressed directly at the strike point, it becomes much more efficient in the region 20-100 mm away from it in the far scrape-off-layer.

1. Introduction

Even in small quantities impurities, i.e. elements other than the hydrogen isotopes, can have a large impact on the performance of a fusion experiment. In particular elements with a large nuclear charge Z can degrade significantly the plasma energy confinement time due to bremsstrahlung and line radiation when penetrating the hot confinement region of a fusion device. High Z materials like tungsten on the other hand withstand excellently the high heat fluxes and reveal small physical sputtering coefficients at a high threshold. For the choice of the wall material in a fusion device several aspects play an important role: (1) the maximum tolerable impurity concentration in the core ($c_C \lesssim 10^{-2}$ for carbon and $c_W \lesssim 10^{-4}$ for tungsten, cf. [1]), (2) the erosion yield of the plasma facing components and (3) the transport in the plasma. Apart from these plasma

physical requirements other mechanical, economic and safety issues have to be taken into account. Carbon for example binds the radioactive tritium chemically, which forbids its usage in a fusion reactor like DEMO. In particular for this reason the experimental proof provided by ASDEX Upgrade (AUG) that high plasma performance can be achieved in a full tungsten device (cf. [2]) was essential. In order to keep the tungsten concentration in the core region below the required level, a high 'divertor retention' R (the definition is given by Eq. 4 below) is required, i.e. a high efficiency of the divertor to suppress the impurity transport from divertor sources to the core region. Geier et al. [3] recently found a value of $R = 17$ experimentally comparing localized injections of gaseous $W(CO)_6$ in the main chamber and in the divertor. Tungsten transport was also studied experimentally and theoretically in several devices like Alcator C-mod and JET [4, 5].
The danger that large amounts of tungsten impurities are released from melting divertor tiles in ITER due to off-normal heat loads motivated experiments with a melting tungsten pin exposed to the AUG divertor plasma close to the outer strike point, on which we reported recently [6, 7]. These experiments showed that even with an almost completely eroding pin ($1\times1\times3$ mm^3) stable discharge conditions can be achieved. However, the melting dynamics, the motion of W droplets ejected from the pin, the ablation of material and the transport in the plasma are all four complex topics and so in this article we focus only on the latter, by simulating the impurity distribution resulting from a point source at different positions in the scape-off layer (SOL). Our main goal is to determine the aforementioned divertor retention R as a function of the source position in the divertor theoretically. Although R is expected to be toroidally symmetric – as long as the magnetic configuration is completely symmetric – we chose a 3D approach for the impurity transport by applying the Edge Monte Carlo 3D (EMC3) Eirene code package for the following two reasons: (1) The impurity distribution in the SOL is a 3D structure and therefore local and line-integrated diagnostics are sensitive to the toroidal source and measurement positions. (2) An experimental validation of the axisymmetric (2D) case is required before addressing the 3D non-axisymmetric situation, for example when simulating the edge plasma under the influence of the (resonant) magnetic perturbation coils recently installed at AUG.
The outline of the paper is the following: In Sec. 2 we will briefly introduce the EMC3-Eirene code package and summarize the issues concerning the construction of the computational grid and the impurity transport simulation. The results of the deuterium bulk plasma transport and that of the impurities are shown in Sec. 3 where we also discuss the dominant mechanism for the spatial dependence of R. A summary and an outlook are finally given in Sec. 4.

2. EMC3-Eirene

2.1. Code and computational grid

EMC3 solves Braginskii's equations (Eqs. 3–6 in Ref. [8]) and is self consistently coupled to Eirene, which solves the kinetic Boltzmann equation for neutral particles [9]. The working principle as well as the full set of equations solved by the EMC3-Eirene code package are described in detail in Ref. [8]. Although a Monte Carlo principle is applied to solve the equations mathematically, it has to be pointed out that EMC3 describes the edge plasma by a fluid approach including all the approximations made in the fluid picture. The application of the Monte Carlo technique is motivated by its high numerical stability and its capability of dealing with stochastic fields. Despite the completely different numerical approach, the different type of computational grid and the less comprehensive set of atomic reactions, benchmarks against SOLPS and UEDGE2D-Eirene have shown a reasonably good agreement with 2D fluid codes recently [10–12] for the axisymmetric case. It has to be mentioned, however, that drifts and volumetric sinks via recombination are not taken into account by EMC3 so far.

An indispensable input for EMC3-Eirene is the computational grid. It not only divides the computational space into finite volumes but also stores the entire magnetic geometry. Formally the grid is divided into N_z zones labeled with the 'zone' index $iz = 0 \dots N_z - 1$. Each zone constitutes a structured cubic grid, meaning that for every 'radial', 'poloidal' and 'toroidal' index $ir = 0 \dots N_r(iz) - 1$, $ip = 0 \dots N_p(iz) - 1$ and $it = 0 \dots N_t(iz) - 1$ a grid vertex $\vec{G}^{iz}_{ir,ip,it}$ exists and that cells with neighboring indices are also neighbors in real space. In toroidal direction the grid is aligned to the field, i.e. grid points with the same iz, ir and ip lie on the same field line. In order to be able to adapt the radial and toroidal resolution according to the strongly anisotropic transport in the plasma, the present grid is also aligned to the flux surfaces, meaning that $\Psi = \text{const.}$ for grid points with the same iz and ir. A precondition for the code is that grid points with the same iz and it lie on the same poloidal plane $\phi = \text{const.}$ Figure 1 shows a poloidal cross-section of a grid for one AUG sector (i.e. $1/16^{th}$ of the torus circumference) consisting of three zones, 'core', scrape-off layer 'SOL' and private flux region 'PFR' at the toroidal position $\phi = 11.25°$. This grid consists of about 500,000 cells, we will also refer to as 'geometrical cells'. Plasma parameters, however, are represented by so-called 'physical cells', i.e. groups of geometrical cells whose resolution is optimized to meet the local requirements. While the very first geometrical cells in front of the targets (where gradients are very steep) are all single physical cells, many cells along a field line in the core region (where parallel transport is large) are grouped together. This technique reduces the number of cells handled by EMC3-Eirene by about a factor of 10 for the AUG grid, which reduces the computational effort to a reasonable level.

2.2. Impurity transport and atomic data

Continuity and momentum balances solved by EMC3 to describe the impurity transport are given in Ref. [8] by Eqs. (7) and (8). These equations are solved for all ionization states. Instead of solving the energy equation for the impurities we assume thermal equilibrium with the plasma background $T_Z = T_i$. In particular for the low ionization state this assumption is questionable. Apart from an experimental verification of our results we also plan a comparison with kinetic codes like DIVIMP [13] or ERO [14]. While the continuity equation is fully equivalent to that of the background plasma, it is assumed that the impurity momentum is governed by classical forces. This simplification is generally used for the tokamak [15]. Dividing Eq. (8) in Ref. [8] by $U_{Ii}^Z = m_Z n_I^Z/\tau$, where τ is the mean impurity-ion collision time, and resolving it with respect to the impurity velocity $V_{I||}^Z$ yields

$$V_{I||}^Z = V_{i||} + \beta_i' \nabla_{||} T_i + \alpha_e' \nabla_{||} T_e - \frac{\tau}{m_Z} \frac{\nabla_{||} n_I^Z T_i}{n_I^Z} + \frac{\tau Z e}{m_Z} E_{||} \tag{1}$$

with $\alpha_e' = \alpha_e \tau/m_Z$ and $\beta_i' = \beta_i \tau/m_Z$, where the dimensionless parameters α_e and β_i are given in Ref. [15]. $V_{i||}$ is the parallel ion streaming velocity, T_e and T_i the electron and ion temperatures, m_Z the impurity atom mass, n_I^Z the impurity density and $E_{||}$ the parallel electric field. As shown later the first two terms on the right hand side of Eq. 1 are the predominant ones to determine $V_{I||}^Z$.

An important prerequisite for the simulation of the plasma, the neutral particle and the impurity transport are reliable atomic data to determine ionization and recombination rates. While very complete and validated databases like ADAS were build up over several decades of research for a variety of materials/elements, tungsten is a far more complex and far less studied element. Here we used recent data for tungsten originating from Loch et al. [16], who carried out atomic calculations applying different theoretical models. The rate coefficients given there were validated against experiments in AUG by Pütterich et al. [17] and partly modified by empirical correction factors.

3. Results

3.1. Simulation of the D plasma bulk

Before the simulation of impurities is addressed we first have to simulate the bulk D plasma as realistically as possible. Here we simulated the AUG L-mode discharge #25460 at 1.7 s. The plasma was heated by $P_{ECRH} = 0.8$ MW of ECRH and $P_{OH} = 0.7$ MW of ohmic power yielding in equilibrium (the stored energy in the core plasma is observed to be constant) a power flux into the edge plasma of about $P_{in} = P_{ECRH} + P_{OH} = 1.5$ MW. The plasma current is $I_p = 1$ MA, the toroidal magnetic field at the magnetic axis $B_t = -2.5$ T and $q_{95} = -4.1$. In order to match the density and temperature profiles measured by the Lithium beam and the electron cyclotron emission (ECE) diagnostics in the main chamber (cf. Fig. 2) we assumed (anomalous) particle and heat diffusion coefficients of $D_{\perp,e} = D_{\perp,i} = 0.25$ m^2/s and

$\chi_{\perp,e} = \chi_{\perp,i} = 2.5$ m^2/s, respectively, a separatrix density of $n_{sep} = 1.2 \cdot 10^{19}$ m^{-3} and that the electrons receive 70% of the heating power ($P_e = 0.7P_{in}$, $P_i = 0.3P_{in}$). The major part of this power is finally deposited on the divertor target plates (where heat sheath transmission coefficients of $\gamma_i = 2.5$ and $\gamma_e = 4.5$ are assumed) while radiation processes of the neutral deuterium and the impurities in the SOL consume another fraction ($P_{rad} \approx 0.4$ MW) of the input energy. Due to the exclusion of impurity radiation in the simulation and the uncertainties in the measured radiation losses and power deposition we cannot expect a perfect agreement between experiment and simulation. However, in order to prove that our conclusions do not depend on the particular values of the external parameters, we repeated the simulation variing the separatrix density and the heating power respectively. Apart from the energy fluxes commonly determined by means of thermography, the particle fluxes measured by the divertor Langmuir probes are of particular importance for the comparison with the experiment. As shown in Fig. 3 the simulated ion saturation currents agree within 25–30% error with the measured ones.

3.2. Tungsten transport simulation

For a fusion device a crucial quantity is the maximum tolerable concentration of impurities in the confinement region. For tungsten it has been shown [1], that ignition conditions cannot be achieved for concentrations $c_W = n_W/n_e \geq 1.2 \times 10^{-4}$, where n_W is the total (sum over all ionization states) tungsten density. In this section we want to simulate which amount of tungsten is found in the core plasma for a given tungsten flux Φ_W from a point source somewhere in the SOL. Being free of impurity sources, n_W is constant in the entire core region under the assumption of purely diffusive transport and therefore equal to the separatrix density, which is directly computed by the impurity part of EMC3-Eirene. In this case the absolute number of tungsten atoms $N_W = n_W V_{core}$ can be calculated from the core volume $V_{core} = 13$ m^3 and their mean residence time in the plasma is given by

$$\tau_W = \frac{N_W}{\Phi_W} \ . \tag{2}$$

The tungsten concentration (averaged over the core volume) can then be determined by

$$c_W = \frac{\Phi_W \tau_W}{V_{core} \overline{n}_e} \ , \tag{3}$$

where $\overline{n}_e$ is the volume averaged electron density in the core. An important quantity is also the so called divertor retention

$$R = \frac{\tau_{W,mc}}{\tau_{W,div}} \ , \tag{4}$$

i.e. the mean residence time $\tau_{W,mc}$ of a main chamber source (in the simulation located at the low-field side on the same height as the magnetics axis) over that of a divertor source $\tau_{W,div}$ as it was defined by Roth and Janeschitz [18]. This number is much easier to determine experimentally since it does not depend on the absolute calibration of the

measurement of the tungsten content in the core. Given that the assumption of constant tungsten core density n_W is not required for the determination of R, but only that N_W scales linearily with n_W at the separatrix, R is also a much more robust number in the simulation.

In our simulations we start neutral tungsten atoms at different poloidal positions s_{inj} relative to the outer strike point s_{sp} about 1 mm in front of the outer divertor target plate at an initial energy of 0.5 eV (corresponding to the energy at the boiling temperature of tungsten) following a cosine distribution in velocity space. As shown in Fig. 4 τ_W and R show a very sensitive dependency on the source to strike point distance $s_{inj}-s_{sp}$. While a very high retention of $R > 1000$ is found directly at the strike point, it rapidly decreases moving only a few cm away from it in particular into the SOL region, where it can even be smaller than one. For understanding this result we analyze the force balance for the impurities, which – converted into velocity units – is given by Eq. 1. Fig. 5 represents the dominant terms of this equation. As shown there the resulting streaming velocity of the impurities (Fig. 5 a) is determined essentially by the streaming velocity of the bulk plasma ions (Fig. 5 b) and a term corresponding to the ion thermal forces (Fig. 5 c). For large parts of the SOL the thermal forces are dominant, which drive the impurities towards the hot main chamber plasma. The retention in this region is very low. In the very first layer in front of the target, where we start the impurities, however, strong recycling takes place and the streaming velocity is close to the speed of sound. Here the Krasheninnikov criterion [19] (that the convective heat transport is larger than the conductive one) is fulfilled and so the friction forces are dominant, which is seen by the thin (2-3 cm in poloidal direction) blue region in front of the outer and the thin red region in front of the inner target. In order to fulfill Eq. 1 strong gradients in the impurity density (and therefore in the impurity pressure) build up to balance the frictional forces.

Let us consider a very simple 1D model for the impurity transport along the field lines in the recycling region, i.e. a few cm in front of the divertor target. We describe the position along the field line by the length coordinate l starting from the target surface. For the model we make the following assumptions: (1) All neutral tungsten atoms are immediately ionized after entering the plasma (in the SOL this is probably a good approximation since the mean free path for the first ionization is $\lambda_{W^0} \leq 0.5$ mm everywhere) while (2) the mean free path length for the second ionization is large with respect to the size l_0 of the considered zone. Consequently, the entire interval $0 < l \leq l_0$ is impurity source free. We furthermore assume (3) constant plasma parameters and neglect the radial transport (4) for the impurities in this interval. Under these conditions we can neglect $V^Z_{I||}$, ∇T_e, ∇T_i, ∇T_Z and E_{II} in Eq. 1 and describe the impurity density by an exponential function $n^Z_I(l) = n^Z_I(0)\exp(-l/\lambda)$, where λ is the decay length

$$\lambda = \frac{\tau T_i}{\left(-V_{i||}\right) m_Z} \ . \tag{5}$$

τ here is the parallel collisional diffusion time given by formula 6.37 in Ref. [15]. Computing the ratio $n^Z_I(l_0)/n^Z_I(0)$ at a characteristic length l_0 given by the size of this

region (where $V_{i||} \approx c_s = \sqrt{T_i(1+\alpha)/m_i}$ and $\alpha = T_e/T_i$) we can deduce a theoretical divertor retention

$$R_{1D} = c_1 \exp\left(c_2 \frac{n_e}{T_i^2}\right) \ . \tag{6}$$

While the first constant c_1, which is determined by the impurity transport outside the considered region, is used as a fitting parameter here, c_2 is given by

$$c_2 = 6.95 \times 10^{-18} \mathrm{m^2 eV^2} l_0 \sqrt{1+\alpha} Z^2 \ln\Lambda \ . \tag{7}$$

Assuming $c_1 = 0.5$, $l_0 = 0.5$ m (corresponding to a poloidal extension of about 20 mm), $Z = 1$, $\alpha \approx 1$ and $\ln\Lambda \approx 10$ (i.e. $c_2 = 5 \times 10^{-17}$ $\mathrm{m^3 eV^2}$) formula 6 was compared to the EMC3-Eirene simulation results shown in Fig. 4 using the values for n_e and T_i at the target. As shown by the blue curve, R_{1D} has a similar shape than the EMC3-Eirene simulations at least for the region above the strike point (i.e. for $s_{inj} > s_{sp}$) which confirms that the dominant mechanism is captured by the model. It has to be pointed out, however, that neither the assumption (2) of a single ionization state of the impurities nor that of constant plasma parameters (3) are good approximations in the interval $0 < l \leq l_0$ so that we cannot expect an accurate agreement. Independently of the numerical value of c_2, however, the exponential dependence on n_e/T_i^2 seems to be a general feature of the divertor retention at the divertor target.

Underneath the strike point (i.e. for $s_{inj} < s_{sp}$) another effect becomes dominant, namely the strong increase of the mean free path for the first ionization. Neutral tungsten atoms can cross the region of strong deuterium fluxes, so that the retention effect is strongly reduced. The mean free path length can even be longer than the distance to the surface of the roof baffle opposite to the injection position. It is not surprising that the result then depends sensitively on the sticking coefficient S_{W^0} on the surface and so we show the two extreme cases $S_{W^0} = 0$ (the neutral tungsten atoms are reflected) and $S_{W^0} = 1$ (the target is a sink for impurities) respectively.

In addition to the spatial dependence of R we also found the transport to be very sensitive to the discharge conditions. Raising artificially the separatrix density by 20% to $n_{e,sep} = 1.6 \times 10^{19}$ $\mathrm{m^{-3}}$ while keeping the heating power constant leads to a strong increase of the collisionality in the SOL which in turn strongly surpresses the tungsten transport to the mainchamber, as one can see clearly in Fig. 6. As shown by the blue curve the spatial dependence of the divertor retention can still be roughly approximated by formula 6, the absolute value, however is significantly higher ($c_1 = 1.5$). A similar effect is achieved by decreasing the input power by 33% to about P=1 MW (this is approximately the input power minus the losses due to impurity radiation). Here again the spatial dependence of the divertor retention is still close to that prediced by formula 6, but with $c_1 = 7.5$. Since the strong spatial dependence of the divertor retention was identified to be a downstream effect, this result remains valid also for H-mode discharges, although the absolute value might be different there.

In order to compute the tungsten concentration (and therefore a global value for the divertor retention) in a real discharge it would be necessary to know the effective source

strength as a function of the divertor coordinate s. There are expressions to compute the sputtering yield as a function of the plasma parameters, like the one given by Bohdansky [20]), however, the main erosion channel is most likely not that from the D bulk plasma but from the low- and medium Z impurities which were not yet addressed by the simulation. In addition to that the mechanism of prompt re-deposition would have to be taken into account, an effect that cannot be addressed by a fluid model like EMC3-Eirene.
As a general statement, however, it remains valid that the best recipe to keep the core tungsten concentration low is to increase collisionality and therefore the frictional forces in the divertor.

4. Summary and outlook

EMC3-Eirene was applied to simulate the D bulk plasma, the deuterium neutral and the tungsten impurity transport in AUG L-mode divertor discharges. The simulation of the deuterium bulk plasma and neutral gas showed good agreement both in the main chamber and in the divertor. The simulated values for the mean tungsten residence time τ_W and the divertor retention R are not incompatible with values found in different experiments [3–7], the simulation, however, showed to be very sensitive on the location of the impurity source relative to the outer strike point and also on the SOL plasma conditions. In particular the transport to the core from sources 20 to 100 mm away from the strike point in the far scrape-off layer is most efficient. The friction forces caused by the strong deuterium bulk plasma fluxes in the recycling region (about 2 cm poloidally in front of the divertor targets) were identified as the dominant term to explain this effect. From a 1D model we derived an exponential dependence on n_e/T_i^2 that approximates the EMC3-Eirene simulations fairly well. Given that the spatial dependency of the divertor retention is mostly determined by the downstream profiles, this effect - at least qualitatively - is also expected for H-modes.
In addition to addressing a more refined and self-consistent simulation of AUG H-modes and the sources in the divertor as a next step it is also planned to re-install in AUG the $W(CO)_6$ injector already used in Ref. [3]. Scanning the strike point to nozzle distance while monitoring the core tungsten concentration, it should be possible to test the sensitive spatial dependency of the divertor retention shown in Figs. 4–7.
A confirmation of these results would have strong implications for the future design of tokamak divertors.

5. References

[1] Neu R. *et al.* 2003 *Fus. Eng. Design* **65** 367–374
[2] Neu R. *et al.* 2009 *Phys. Scr.* **T138** 014038
[3] Geier A. *et al.* 2002 *Plasma Phys. Contr. Fus.* **44** 2091
[4] Barnard H.S. *et al.* 2011 *J. Nucl. Mater.* **415** S301–4
[5] Strachan J.D. *et al.* 2010 *J. Nucl. Mater.* **415** S501–4

[6] Krieger K. *el al.* 2011 *J. Nucl. Mater.* **415** S297–300
[7] Lunt T. *el al.* 2011 *J. Nucl. Mater.* **415** S505–8
[8] Feng Y. *et al.* 2004 *Contrib. Plasma Phys.* **44**, No. 1–3, 57–69
[9] Reiter D. *et al.* 2005 *Fus. Sci. Tec.* **47** 172–186
[10] Lunt T. *el al.* 2009 36^{th} EPS Conference on Plasma Phys. Sofia, June 29 - July 3, 2009 ECA Vol.33E, P-1.154
[11] Harting D. *el al.* 2011 *J. Nucl. Mater.* **415** S540–4
[12] Feng Y. *el al.* 2011 38^{th} EPS 2011 Conference on Plasma Phys. Strasbourg, June 27 - July 1, P1.071
[13] Stangeby P., Elder J. 1992 *J. Nucl. Mater.* **258** 196–198
[14] Naujoks D. *el al.* 1994 *J. Nucl. Mater.* **210** 43–50
[15] Stangeby P.C. 2000 *The Boundary of Magnetic Fusion Devices*, *IOP Publishing*, Bristol
[16] Loch S. D. *et al.* 2005 *Phys. Rev. A* **72** 052716
[17] Pütterich T. *et al.* 2008 *Plasma Phys. Contr. Fus.* **50** 085016
[18] Roth J., Janeshitz G. 1989 *Nucl. Fusion* **29**, No. 6, 915–935
[19] Krashenninikov S. I. *et al.* 1991 *Nucl. Fusion* **31** 1455–1470
[20] Bohdansky J. 1984 *Nucl. Instr. and Meth. B* **2** 587

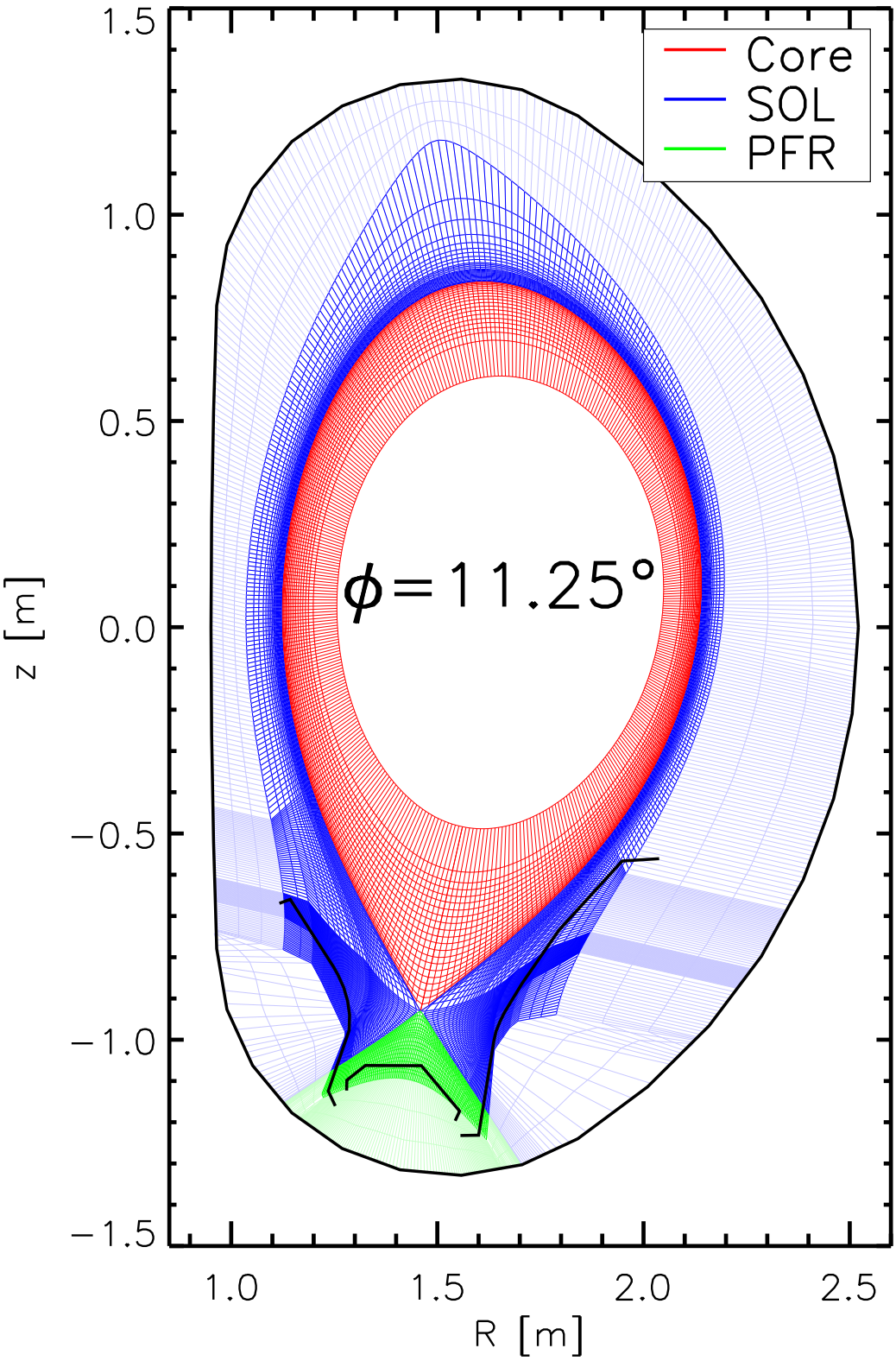

Figure 1. Cross section of the computational grid at $\phi = 11.25°$ used by EMC3-Eirene to simulate the AUG divertor discharge #25460 at 1.7 s. The grid is extended in the third dimension along the field lines to cover the poloidal angle of $\phi = 0 \ldots 22.5°$, i.e. one 'sector' of AUG.

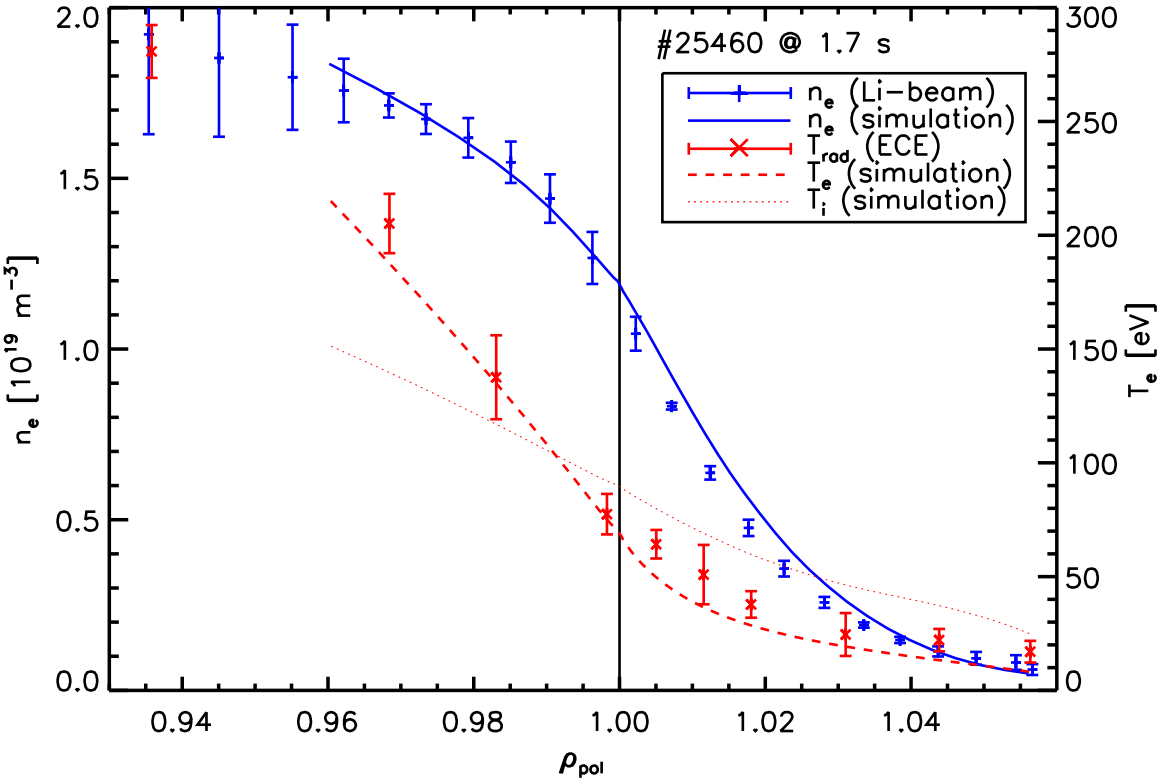

Figure 2. Density (blue) and temperature (red) profiles of the AUG L-mode discharge 25460 at 1.7 s in the main chamber as measured by the Li-beam and by the electron cyclotron emission (ECE) diagnostics (data points) and simulated by EMC3-Eirene (lines).

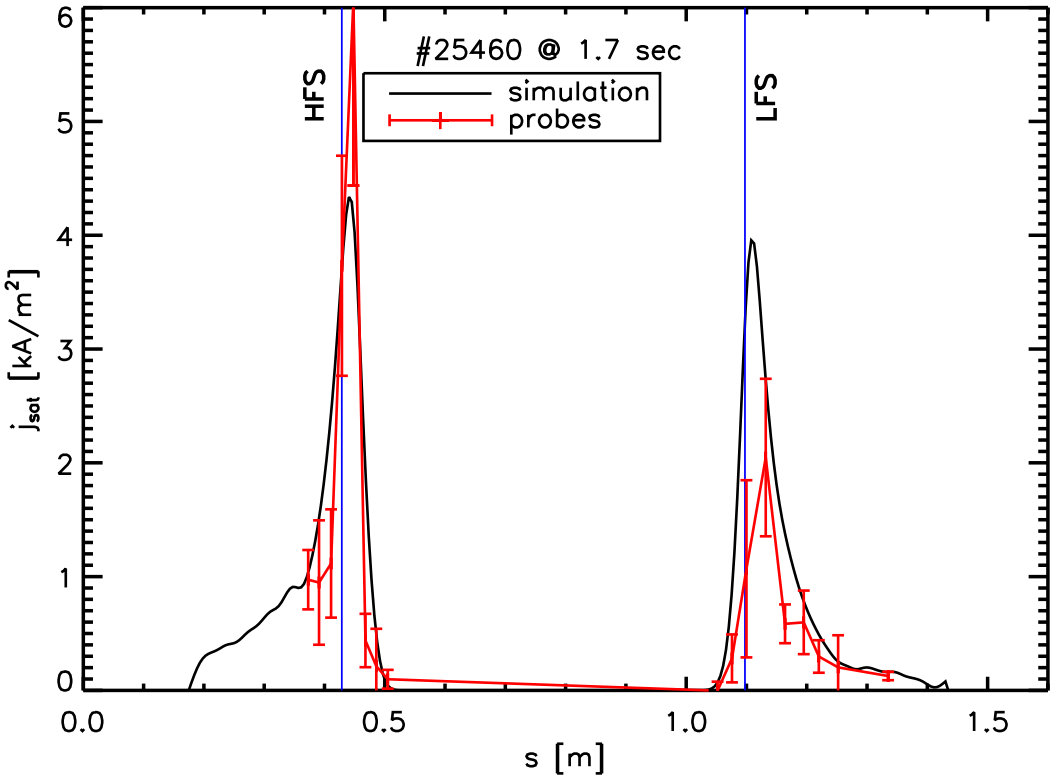

Figure 3. Ion saturation current density at the divertor target plates measured by Langmuir probes (red data points) compared to the simulation of EMC3-Eirene (black curve). s defines the position along a curved path following the divertor contour, the blue vertical lines indicate the nominal strike point positions.

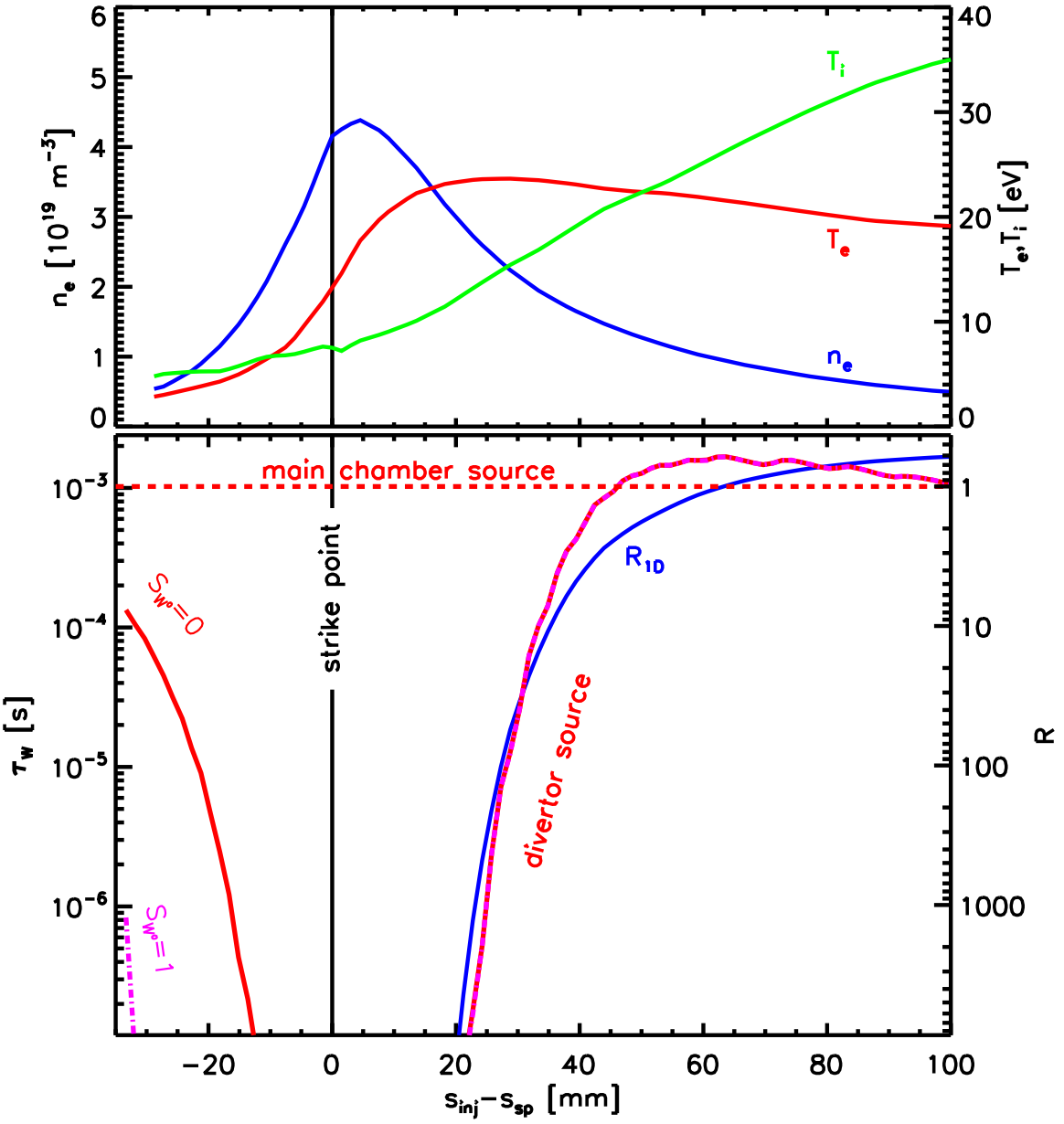

Figure 4. Top: n_e and T_e profiles close to the outer divertor target of the L-mode discharge #25460 at 1.7 s. The separatrix density was $n_{e,sep} = 1.3 \times 10^{19}$ m^{-3}. Bottom: simulated mean tungsten residence time τ_W as a function of the injection position $s - s_{sp}$ relative to the outer strike point. The solid and the dash-dotted lines compare the cases with a sticking coefficient of $S_{W^0} = 0$ and $S_{W^0} = 1$, respectively. With an average core density of $\overline{n}_e = 3.4 \times 10^{19}$ m^{-3} and Eq. 3 the core concentration can be determined for a given influx Φ_W. The right scale shows the divertor retention defined in Eq. 4. The blue curve shows Eq. 6 with $c_1 = 1$ and $c_2 = 5.0 \times 10^{-17}$ m^{3}eV^2 obtained from a simple 1D model.

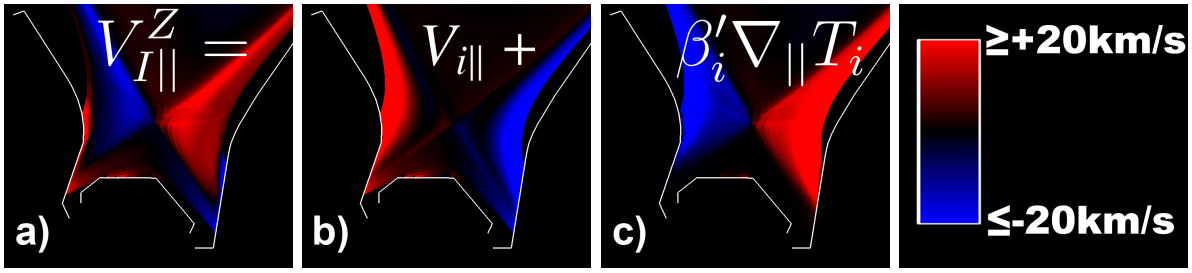

Figure 5. 'Force balance' for the tungsten impurities. The three plots a),b) and c) represent the corresponding terms in Eq. 1.

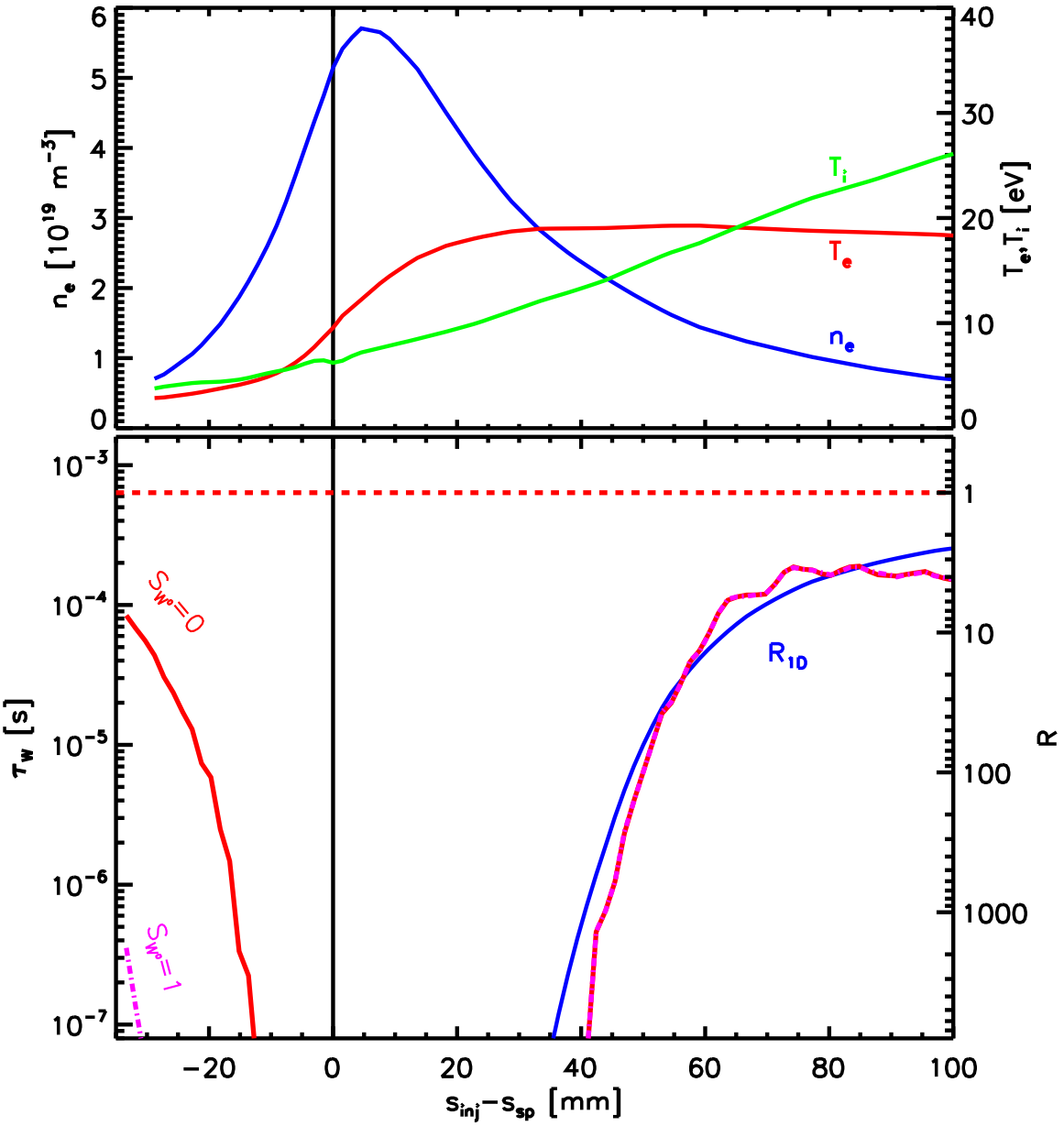

Figure 6. Same as Fig. 4 but for a separatrix density of $n_{e,sep} = 1.6 \times 10^{19}$ m^{-3}. In contrast to Fig. 4, the blue curve was evaluated for $c_1 = 4$.

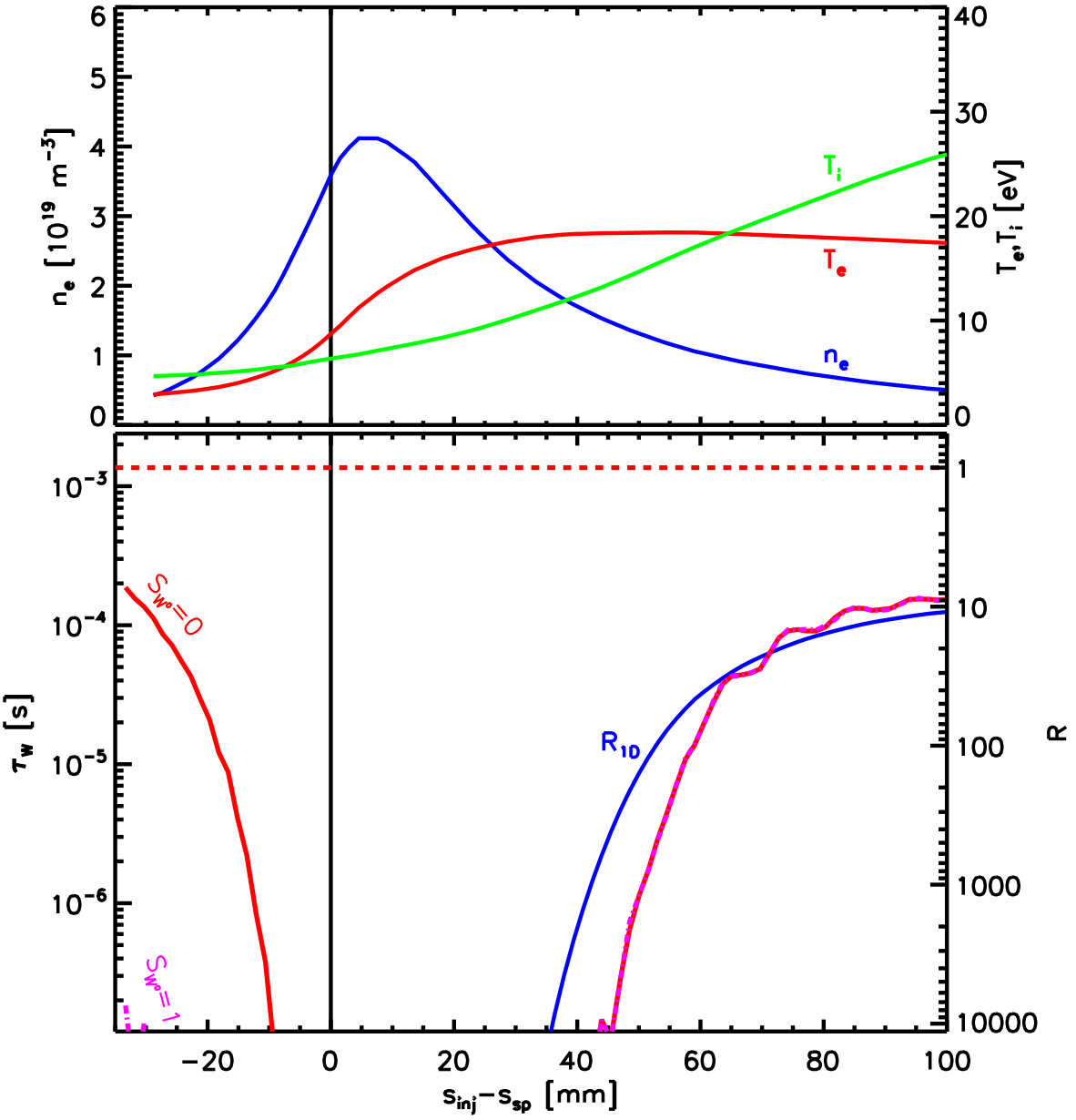

Figure 7. Same as Fig. 4 but with about 50% less heating power, i.e. $P_{heat} = 1.0$ MW. In contrast to Fig. 4, the blue curve was evaluated for $c_1 = 15$.